

Figure 2. Dc cyclic voltammetry of microperoxidase (0.5 mg/mL) in $\text{Mg}(\text{ClO}_4)_2$ (0.025 M) and phosphate buffer (0.02 M) at pH 7.0, in the potential range 0 to -0.60 V vs SCE; sweep rate: (a) 20; (b) 50; (c) 100; (d) 200 mV/s. Temperature: 25 °C. Inset shows a plot of i_p vs (scan rate) $^{1/2}$.

to aggregation of oxidized or reduced microperoxidase was obtained.

It has been reported^{3,5} that Mg^{2+} acts as a promoter for the electron-transfer process by forming a transient bridge between a negatively charged macromolecule and the electrode surface. Since both microperoxidase at neutral pH ($\text{pI} = 4.7$) and the glassy carbon surface, under the experimental conditions employed,^{12,13} are negatively charged, the role of Mg^{2+} has been investigated. Dc cyclic voltammograms of microperoxidase in the presence of 25 mM Mg^{2+} , shown in Figure 2, indicate a reversible electrode process. Under these conditions, both the cathodic and anodic waves are better resolved with respect to the experiments carried out in 100 mM Na^+ , and the electron-transfer reaction is reversible, ($i_{pa}/i_{pc} \approx 1$). As expected, these results demonstrate some role of the electrostatic interactions in controlling the formation of a favorable transient complex between the electrode surface and the heme-peptide; given the negative charge of microperoxidase at neutral pH, the presence of divalent ions (e.g., Mg^{2+}) surely facilitates electron transfer. Even under these conditions, the process is diffusion-controlled (see inset of Figure 2); the calculated diffusion coefficient and rate constant have values similar to those obtained in the presence of 100 mM Na^+ . Thus, Mg^{2+} affects only some aspects of the electrochemistry of microperoxidase, such as the reversibility, while the electron-transfer rate remains unaffected.

It has been reported⁸ that the microperoxidase-imidazole complex exists in solution as monomer, independent of pH, while unliganded microperoxidase tends to aggregate at alkaline pH. Therefore, cyclic voltammograms were also obtained in the presence of 50 mM imidazole, which coordinates as a ligand of the heme iron. The results (not shown) in the presence of Na^+ or Mg^{2+} were very similar to those illustrated in Figures 1 and 2, respectively; moreover, in accordance to what was reported by Harbury and Loach in their potentiometric studies on the same system,⁸ a more negative value for $E_{1/2}$ (-200 ± 5 mV) was obtained.

Microperoxidase, the undecapeptide of cytochrome *c* with molecular mass of about 1900, represents a good system to study the reversibility of the reaction at the electrode surface, and it is a source of information on the electrochemical behavior of the heme iron when unshielded by a large polypeptide, as it happens in the case of all hemoproteins. For metalloproteins, rapid electron transfer at the electrode is best achieved in the presence of appropriate promoters, such as 4-4' bipyridyl for cytochrome *c*,² which increase the electron-transfer rate by favoring correct

orientation of the metalloprotein. Cyclic voltammetry of microperoxidase shows that rapid, reversible electron transfer at the electrode is achieved even in the absence of mediators or promoters. Of course, this behavior is to be associated with the simpler and disordered conformation of microperoxidase in which the heme, more exposed to the solvent, is facilitated to exchange electrons. Thus, these results strongly support the notion that, in metalloproteins, a buried metal site is the major hindrance to a rapid reversible electrochemical behavior. Under appropriate conditions, the exposed heme of microperoxidase may serve the role of a specific promoter between the electrode surface and metalloproteins in solution.

The redox potentials determined for microperoxidase are in good agreement with previous data obtained by Harbury and Loach⁸ by potentiometry. Comparison with these results shows that cyclic voltammetry is extremely rapid, does not require the use of mediators or stepwise addition of reductants, and yields additional information on reversibility and rates of electron transfer.

The negative $E_{1/2}$ values of microperoxidase provide additional evidence for the significance of the degree of exposure of the heme to the solvent in affecting its redox potential. In fact, a higher degree of heme exposure lowers the redox potential of a hemo-protein,¹⁴ as recently confirmed by an electrochemical investigation on carboxymethylated cytochrome *c*, whose redox potential ($E_{1/2} = -250$ mV vs NHE) was found to be approximately 0.5 V lower than that of native cytochrome *c* ($E_{1/2} = +250$ mV).¹⁵

Acknowledgment. We are grateful to Prof. H. A. O. Hill for valuable suggestions.

Registry No. Microperoxidase, 30975-71-4.

(14) Stellwagen, E. *Nature (London)* **1978**, *275*, 73-74.

(15) Di Marino, M.; Santucci, R.; Brunori, M.; Ascoli, F.; Marassi, R. *Bioelectrochem. Bioenerg.* **1987**, *17*, 27-34.

Potential Building Blocks for Molecular Ferromagnets: $[\text{Mn}_{12}\text{O}_{12}(\text{O}_2\text{CPh})_{16}(\text{H}_2\text{O})_4]$ with a $S = 14$ Ground State

Peter D. W. Boyd,^{1a} Qiaoying Li,^{1b} John B. Vincent,^{2a} Kirsten Foltling,^{2b} Hsiu-Rong Chang,^{1b} William E. Streib,^{2b} John C. Huffman,^{2b} George Christou,^{*,†,2a} and David N. Hendrickson^{*,1b}

School of Chemical Sciences, University of Illinois Urbana, Illinois 61801
Department of Chemistry and the Molecular Structure Center, Indiana University Bloomington, Indiana 47405
Received August 24, 1988

Several groups are currently trying to prepare ferromagnetic organic,³⁻⁸ organometallic,⁹ and inorganic¹⁰⁻¹² materials. Mataga

[†] Alfred P. Sloan Research Fellow, 1987-1989. Camille and Henry Dreyfus Teacher-Scholar, 1987-1992.

(1) (a) On sabbatical leave at the University of Illinois from the Chemistry Department, University of Auckland, Auckland, New Zealand. (b) University of Illinois.

(2) (a) Indiana University, Chemistry Department. (b) Indiana University, Molecular Structure Center.

(3) Torrance, J. B.; Oostra, S.; Nazzari, A. *Synth. Met.* **1986**, *19*, 709.

(4) Korshak, Yu.; Medvedeva, T. V.; Ovchinnikov, A. A.; Spectro, V. N. *Nature (London)* **1987**, *326*, 370.

(5) (a) Iwamura, H. *Pure Appl. Chem.* **1986**, *58*, 187. (b) Sugawara, T.; Bandow, S.; Kimura, K.; Iwamura, H.; Itoh, K. *J. Am. Chem. Soc.* **1986**, *108*, 368.

(6) Dormann, E.; Nowak, M. J.; Williams, K. A.; Angus, R. O., Jr.; Wudl, F. *J. Am. Chem. Soc.* **1987**, *109*, 2594.

(7) Radhakrishnan, T. P.; Soos, Z. G.; Endres, H.; Azevedo, L. J. *J. Chem. Phys.* **1986**, *85*, 1126.

(8) LePage, T. J.; Breslow, R. *J. Am. Chem. Soc.* **1987**, *109*, 6412.

(9) Miller, J. S.; Epstein, A. J.; Reiff, W. M. *Acc. Chem. Res.* **1988**, *21*, 114 and references therein.

(12) Radin, J. P.; Yeager, E. J. *Electroanal. Chem.* **1972**, *36*, 257-276.

(13) Armstrong, F. A.; Hill, H. A. O.; Walton, N. J. *Quart. Rev. Biophys.* **1986**, *18*, 261-322.

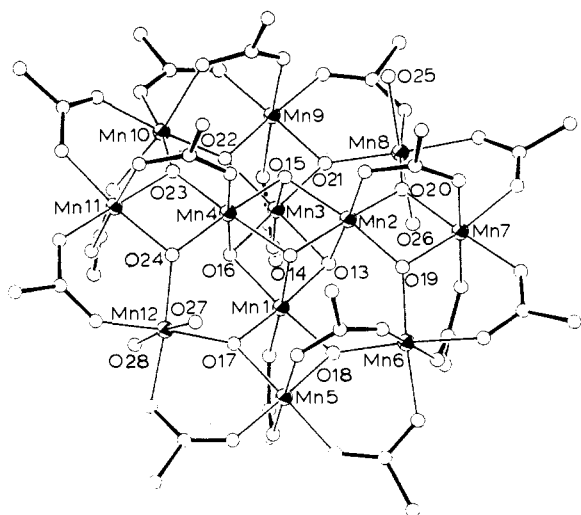


Figure 1. The structure of $[\text{Mn}_{12}\text{O}_{12}(\text{O}_2\text{CPh})_{16}(\text{H}_2\text{O})_4]$. For clarity, the phenyl rings are omitted except for the carboxylate-bound carbon atoms. To avoid congestion, not all oxygen atoms are labeled. See Supplementary Material for a fully labeled figure and a listing of metric parameters.

proposed a method for preparing ferromagnets based on intramolecular ferromagnetic interactions in large molecules.¹³ Several organic^{5,8} and a few inorganic¹² molecules have been reported which have ground states with large spin values. Very recently Caneschi et al.¹² reported a $\text{Mn}^{\text{II}}_6(\text{radical})_6$ complex which has the largest ground-state spin value for any molecule, $S = 12$. In this communication we report the preparation and characterization of a $\text{Mn}^{\text{IV}}_4\text{Mn}^{\text{III}}_8$ molecule which has a $S = 14$ ground state.

$\text{Mn}(\text{OAc})_2 \cdot 4\text{H}_2\text{O}$ (2.00 g, 8.15 mmol) and benzoic acid (7.50 g, 61 mmol) were dissolved in pyridine (20 mL), and solid NBu_4MnO_4 (1.14 g, 3.15 mmol) was added in small portions with stirring to give a dark brown solution. After 15 min, the solvent was removed in vacuo to give a brown oil. This was extracted with EtOH (100 mL) to give a reddish brown solution and a brown solid, which after filtration was extracted into a minimum of CH_3CN and filtered, and the filtrate was allowed to concentrate by slow evaporation to give dark brown crystals of $[\text{Mn}_{12}\text{O}_{12}(\text{O}_2\text{CPh})_{16}(\text{H}_2\text{O})_4]$ (**1**) in 5–10% yield.^{14,15} Complex **1** does hydrolyze in water.

Complex **1** (Figure 1) consists of a central $\text{Mn}^{\text{IV}}_4\text{O}_4$ cubane held within a nonplanar ring of eight Mn^{III} atoms by eight μ_3 -oxide atoms.¹⁶ Peripheral ligation is by 16 μ_2 -benzoate and four H_2O groups. Octahedral Mn^{III} should be Jahn–Teller distorted, and this is apparent in Mn atoms Mn(5–12) with elongation along the axes parallel to the unique molecular C_2 axis. The four H_2O ligands are localized on only two Mn atoms, Mn(8) and Mn(12). Alternatively, the structure of **1** can be considered as the result of fusing together four $[\text{Mn}_4\text{O}_2]$ butterfly units akin to that found¹⁷

(10) Day, P. J. *Magn. Magn. Mater.* **1986**, 54–57, 1442.

(11) (a) Pei, Y.; Verdaguer, M.; Kahn, O.; Sletten, J.; Renard, J. P. *J. Am. Chem. Soc.* **1986**, 108, 7428. (b) *Inorg. Chem.* **1987**, 26, 138. (c) *J. Am. Chem. Soc.* **1988**, 110, 782.

(12) Caneschi, A.; Gatteschi, D.; Laugier, J.; Rey, P.; Sessoli, R.; Zanchini, C. *J. Am. Chem. Soc.* **1988**, 110, 2795.

(13) Mataga, N. *Theor. Chim. Acta* **1968**, 10, 372.

(14) Anal. Calcd for $\text{C}_{112}\text{H}_{88}\text{O}_{48}\text{Mn}_{12}$: C, 47.0; H, 3.1; Mn, 23.0. Found: C, 47.7; H, 3.5; Mn, 22.3.

(15) Crystallographic data at -146°C : triclinic, space group $P\bar{1}$; $a = 27.072$ (19) Å, $b = 17.046$ (11) Å, $c = 14.254$ (8) Å, $\alpha = 98.39$ (3)°, $\beta = 98.44$ (4)°, $\gamma = 89.27$ (4)°, $Z = 2$; $R = 0.0954$, $R_w = 0.1007$ using 4814 reflections with $F > 3.00\sigma(F)$. All non-hydrogen atoms were readily located. Due to the large number of independent atoms (172), the small amount of data, and computer program space limitations, no attempt to locate or include hydrogen atoms was made, and no atoms were refined with anisotropic thermal parameters.

(16) The structure of **1** is similar but not identical with that of $[\text{Mn}_{12}\text{O}_{12}(\text{OAc})_{16}(\text{H}_2\text{O})_4]$ communicated in the following: Lis, T. *Acta Crystallogr., Sect. B* **1980**, B36, 2042.

(17) (a) Vincent, J. B.; Christmas, C.; Huffman, J. C.; Christou, G.; Chang, H.-R.; Hendrickson, D. N. *J. Chem. Soc., Chem. Commun.* **1987**, 236. (b) Vincent, J. B.; Christmas, C.; Chang, H.-R.; Li, Q.; Boyd, P. W.; Huffman, J. C.; Hendrickson, D. N.; Christou, G. Submitted for publication.

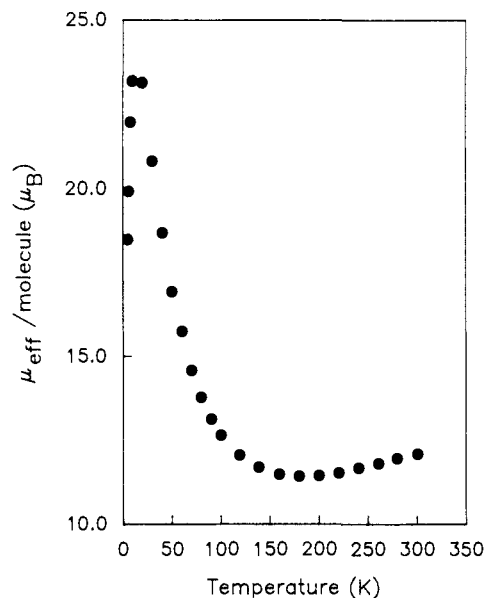


Figure 2. Plot of effective magnetic moment per molecule ($\mu_{\text{eff}}/\text{molecule}$) measured at 10 kG versus temperature for $[\text{Mn}_{12}\text{O}_{12}(\text{O}_2\text{CPh})_{16}(\text{H}_2\text{O})_4]$.

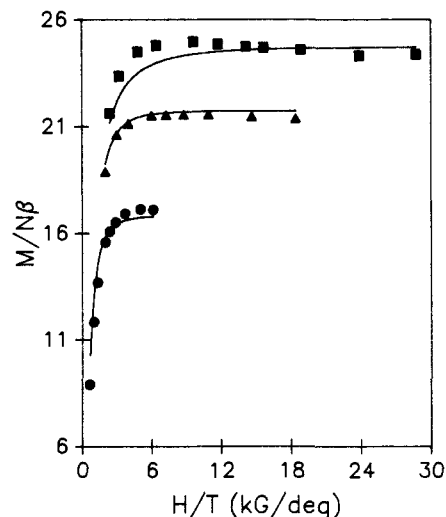


Figure 3. Plot of reduced magnetization, $M/N\beta$ versus H/T for $[\text{Mn}_{12}\text{O}_{12}(\text{O}_2\text{CPh})_{16}(\text{H}_2\text{O})_4]$, where N is Avogadro's number, β is the Bohr magneton, and H is the magnetic field. The data are plotted in three isofield (\bullet , 10 kG; \blacktriangle , 30 kG; and \blacksquare , 48 kG) lines. The solid lines illustrate the result of a least-squares fit of the data to the spin Hamiltonian for a $S = 14$ state experiencing axial and rhombic zero-field splitting.

in the discrete complex $[\text{Mn}_4\text{O}_2(\text{OAc})_7(\text{bipy})_2]^+$.

Magnetic susceptibility data were measured at 10 kG in the range of 5.0–300.8 K for a polycrystalline sample of **1**. Figure 2 shows that the effective magnetic moment per molecule at 300.8 K is $12.10 \mu_B$, which gradually increases with decreasing temperature to reach a maximum of $23.22 \mu_B$ at 10 K, below which it drops to $18.48 \mu_B$ at 5.0 K. In analogy to the data presented by Caneschi et al.¹² the $\mu_{\text{eff}}/\text{molecule}$ data for **1** clearly indicate that there are intramolecular ferromagnetic exchange interactions present in **1**. Furthermore, the shape of the $\mu_{\text{eff}}/\text{molecule}$ versus temperature curve strongly suggests that all of the molecules are in some large-spin ground state at low temperatures. The drop in $\mu_{\text{eff}}/\text{molecule}$ below 10 K likely reflects zero-field splitting in the ground state. No hysteresis effects were seen.

Bulk magnetization (M) measurements were performed for complex **1** in the range of 1.63 to 20 K in fields of 10, 30, or 48 kG to determine the spin of the ground state. The bulk reduced magnetization ($M/N\beta$) is shown in Figure 3, plotted as a function of H/T . The data are plotted as three isofield lines. For a

molecule with all of its population in a ground state with spin S , a plot of $M/N\beta$ versus H/T would follow a Brillouin function¹⁸ and approach a maximum (saturation) value of $2S$ at large values of H/T . The fact that the three isofield lines for complex **1** do not superimpose reflects the presence of zero-field splitting in the ground state.

Least-squares fitting of the $M/N\beta$ versus H/T data for **1** were carried out. At high fields and low temperatures, a true powder average of the theoretically calculated magnetization for all orientations must be made^{19,20} using eq 1. In eq 1, θ and ϕ are

$$\bar{M} = \frac{-N}{4\pi} \int_{\theta=0}^{\pi} \int_{\phi=0}^{2\pi} \left[\sum_{i=1}^p \left(\frac{\delta E_i}{\delta H} \right) \exp(-E_i/kT) / \sum_{i=1}^p \exp(-E_i/kT) \right] \sin \theta d\theta d\phi \quad (1)$$

the polar angle orientations of the field with respect to the molecular principal axis system and $\delta E_i/\delta H$ is the change in the energy of the i th level in response to a change in a magnetic field. The energies of the various sublevels of the ground state are obtained by diagonalization of the $(2S + 1) \times (2S + 1)$ Hamiltonian matrix which includes the Zeeman terms. The derivatives $\delta E_i/\delta H$ were calculated from the corresponding eigenvectors with the Hellman-Feynman theorem.^{19,20} The integral in eq 1 was evaluated numerically.

Thus, the magnetization data for **1** were least-squares fit with the spin Hamiltonian for $S = 14$ including axial ($D\hat{S}_z^2$) and rhombic [$E(\hat{S}_x^2 - \hat{S}_y^2)$] zero-field interactions. TIP was assumed to be 2400×10^{-6} cgsu per complex **1**. For each setting of the parameters (g , D , and E) a powder-average of $M/N\beta$ versus H/T is calculated, and per the simplex approach a least-squares fitting was carried out for the $S = 14$ case which required ~ 35 h of cpu time on a VAX/780 computer. The fitting parameters for $S = 14$ were found to be $g = 1.974$, $D = -0.16 \text{ cm}^{-1}$, and $E = 0.033 \text{ cm}^{-1}$. The solid lines in Figure 3 show that these parameters fit the data well.

In a similar fashion the magnetization data for **1** were fit with the Hamiltonian for either $S = 13$ or $S = 15$. The parameters resulting from these fits are in the format (g , D , E) = (2.121, -0.18, 0.037) and (1.846, -0.138, 0.029), respectively. All three fits are of comparable quality with only the parameter g varying appreciably. The g value for the ground state of a $\text{Mn}^{\text{IV}}\text{Mn}^{\text{III}}_8$ complex should be $2.0 \geq g \geq 1.9$. We conclude that complex **1** has a $S = 14$ ground state and the largest spin ground state yet observed.

The present results indicate that polynuclear manganese complexes are good candidates to exhibit intramolecular ferromagnetic interactions. In fact, very recently we reported²¹ that a distorted cubane $\text{Mn}^{\text{IV}}\text{Mn}^{\text{III}}_3$ complex has a $S = 9/2$ ground state. Clearly a strategy to prepare molecular ferromagnets would be to chemically link together these ferromagnetic molecular building blocks.

Acknowledgment. This work was supported by NIH Grant HL-13652 (D.N.H.) and NSF Grant CHE-8507748 (G.C.). We thank the Bloomington Academic Computing Service for a gift of computer time.

Supplementary Material Available: Fully labeled figure of $[\text{Mn}_{12}\text{O}_{12}(\text{O}_2\text{CPh})_{16}(\text{H}_2\text{O})_4]$ and tables of fractional coordinates, isotropic and anisotropic thermal parameters, and bond distances and angles (10 pages). Ordering information is given on any current masthead page.

(18) Carlin, R. L. *Magnetochemistry*. Springer-Verlag: Berlin, 1986.

(19) Boyd, P. D. W.; Martin, R. L. *J. Chem. Soc., Dalton Trans.* 1979, 92.

(20) Gerloch, M.; McMeeking, R. F. *J. Chem. Soc., Dalton Trans.* 1975, 2443.

(21) Li, Q.; Vincent, J. B.; Libby, E.; Chang, H.-R.; Huffman, J. C.; Boyd, P. D. W.; Christou, G.; Hendrickson, D. N. *Angew. Chem., Int. Ed. Engl.*, in press.

Isolation and Structure of Combretastatin D-1: A Cell Growth Inhibitory Macrocyclic Lactone from *Combretum caffrum*^{1a}

George R. Pettit,* Sheo Bux Singh, and Margaret L. Niven^{1b}

Cancer Research Institute and
Department of Chemistry, Arizona State University
Tempe, Arizona 85287-1604

Received July 13, 1988

The South African tree *Combretum caffrum* (Combretaceae) has been found to contain a series of biosynthetically related substances that significantly inhibit growth of the U.S. National Cancer Institute's murine P-388 lymphocytic leukemia cell line (PS system). Some of these dihydrostilbenes, *cis*-stilbenes, phenanthrenes, and dihydrophenanthrenes, especially combretastatin A-1 and A-4, were also found to strongly inhibit tubulin polymerization.² We now report the isolation and structural elucidation of an unexpected and unusual macrocyclic lactone designated combretastatin D-1 (**1**) with PS cell line activity corresponding to ED_{50} 3.3 $\mu\text{g}/\text{mL}$.

The methylene chloride-methanol extract obtained from 77 kg of *Combretum caffrum* stem wood was initially separated as previously described,^{2a,b} and the fraction that led to combretastatin A-2 was further separated guided by PS bioassay with a sequence of gel permeation, partition (Sephadex LH-20, hexane-toluene-methanol, 3:1:1), and silica gel flash chromatography employing hexane-chloroform-acetone (3:2:0.25) as eluent to afford combretastatin D-1 (**1**) in $2.3 \times 10^{-4}\%$ yield: 180 mg as needles from acetone-hexane: mp 180-181 °C, R_f 0.44 (SiO₂ plate; 1:1 hexane-ethyl acetate); $[\alpha]_D^{25} -100^\circ$ (c 0.015, CHCl₃), HREIMS (m/z) 312.0998 (M^+ , 100%, for C₁₈H₁₆O₅, calcd 312.0998), 267.1015 (M^+ , -CO₂H, 22%), 253.0862 (M^+ - CH₃CO₂, 42%), 227.0712 (M^+ - C₄H₈O₂, 66%), 131.0496 (15%), 122.0368 (6%), and 119.0497 (10%). UV (CHCl₃) λ_{max} 224 (ϵ 15215), 278 (3068) nm; IR (NaCl) ν_{max} 3439, 3431, 3422, 3415, 1735, 1518, 1507, 1438, 1362, 1288, 1216, 1159, and 1142 cm⁻¹. Consult ref 3 for the ¹³C NMR and ¹H NMR assignments.

Mass spectral analysis of lactone **1** revealed molecular formula C₁₈H₁₆O₅ with eleven double bond equivalents. Because of the absence of any isolated or conjugated double bonds, with the exception of two aromatic rings, it became apparent that this molecule possessed two additional rings and a lactone (IR: 1735 cm⁻¹). One ring was located as an epoxide, while the other formed the skeletal cyclic system. The ¹H NMR spectrum was assigned by using ¹H, ¹H COSY techniques. Four isolated coupling patterns were observed. Long-range (five bonds) coupling was observed between H-16 (both α and β) and H-13. All the protons were further assigned on the basis of NOE experiments (cf. **1**; magnitude of observed NOE's were 1 \rightarrow 6%). Proton-20 (δ 4.940) was correlated to δ 112.24 in the carbon spectrum (¹H, ¹³C COSY).

(1) (a) Antineoplastic Agents 160: for the preceding part refer to the following: Warren, B. S.; Herald, C. L.; Pettit, G. R.; Blumberg, P. M. *Cancer Res.*, in press. (b) Department of Chemistry, University of Cape Town, Rondebosch 7700, South Africa.

(2) (a) Pettit, G. R.; Singh, S. B.; Niven, M. L.; Hamel, E.; Schmidt, J. M. *J. Nat. Prod.* 1987, 50, 119. (b) Pettit, G. R.; Singh, S. B. *Can. J. Chem.* 1987, 65, 2390. (c) Pettit, G. R.; Singh, S. B.; Niven, M. L.; Schmidt, J. M. *Can. J. Chem.* 1988, 66, 406. (d) Pettit, G. R.; Singh, S. B.; Schmidt, J. M.; Niven, M. L.; Hamel, E.; Lin, C. M. *J. Nat. Prod.* 1988, 51, 517. (e) Pettit, G. R.; Singh, S. B.; Lin, C. M.; Hamel, E.; Alberts, D.; Garcia-Kendall, D. *Experientia* 1988, in press.

(3) ¹³C NMR (100 MHz, δ , CDCl₃) 26.97 (C-15), 31.24 (C-16), 52.99 (C-3), 55.84 (C-4), 62.56 (C-2), 112.24 (C-20), 115.38 (C-12), 122.03 (C-13), 123.14 (C-19), 123.95 (C-7), 126.34 (C-18), 128.83 (C-6), 131.90 (C-5), 132.44 (C-14), 142.62 (C-11), 149.09 (C-10), 156.01 (C-8), and 172.53 (C-17) ppm; ¹H NMR (400 MHz, δ , CDCl₃) 2.134 (1 H, ddd, $J = 17.5$, 12.5, 1.5 Hz, H-16 α), 2.398 (1 H, ddd, $J = 17.5$, 6.0, 1.50 Hz, H-16 β), 2.583 (1 H, dd, $J = 16.8$, 6.0 Hz, H-15 α), 3.112 (1 H, dd, $J = 16.8$, 12.5 Hz, H-15 β), 3.483 (1 H, ddd, $J = 9.2$, 4.5, 4.5 Hz, H-3), 3.871 (1 H, dd, $J = 12.0$, 9.2 Hz, H-2 α), 4.264 (1 H, dd, $J = 12.0$, 4.5 Hz, H-2 β), 4.355 (1 H, d, $J = 4.5$ Hz, H-4), 4.940 (1 H, d, $J = 1.8$ Hz, H-20), 5.486 (1 H, br s, OH), 6.617 (1 H, ddd, $J = 8.2$, 1.8, 1.5 Hz, H-13), 6.836 (1 H, d, $J = 8.0$ Hz, H-12), 7.081 (1 H, dd, $J = 8.0$, 2.0 Hz, H-19), 7.104 (1 H, dd, $J = 8.0$, 2.0 Hz, H-7), 7.362 (1 H, dd, $J = 8.0$, 2.0 Hz, H-18), 7.549 (1 H, dd, $J = 8.0$, 2.0 Hz, H-6).